Med Microbiol Immunol (2016) 205:209–218
DOI 10.1007/s00430-015-0441-y

ORIGINAL INVESTIGATION

Enhanced growth of influenza A virus by coinfection with human parainfluenza virus type 2

Hideo Goto[1] · Hironobu Ihira[1] · Keiichi Morishita[1] · Mitsuki Tsuchiya[1] · Keisuke Ohta[1] · Natsuko Yumine[1] · Masato Tsurudome[2] · Machiko Nishio[1]

Received: 13 October 2015 / Accepted: 8 November 2015 / Published online: 18 November 2015

Abstract It has been reported that dual or multiple viruses can coinfect epithelial cells of the respiratory tract. However, little has been reported on in vitro interactions of coinfected viruses. To explore how coinfection of different viruses affects their biological property, we examined growth of influenza A virus (IAV) and human parainfluenza virus type 2 (hPIV2) during coinfection of Vero cells. We found that IAV growth was enhanced by coinfection with hPIV2. The enhanced growth of IAV was not reproduced by coinfection with an hPIV2 mutant with reduced cell fusion activity, or by ectopic expression of the V protein of hPIV2. In contrast, induction of cell fusion by ectopic expression of the hPIV2 HN and F proteins augments IAV growth. hPIV2 coinfection supported IAV growth in cells originated from the respiratory epithelium. The enhancement correlated closely with cell fusion ability of hPIV2 in those cells. These results indicate that cell fusion induced by hPIV2 infection is beneficial to IAV replication and that enhanced viral replication by coinfection with different viruses can modify their pathological consequences.

Keywords Influenza A virus · Human parainfluenza virus type 2 · Coinfection · Cell fusion

✉ Machiko Nishio
mnishio@wakayama-med.ac.jp

[1] Department of Microbiology, School of Medicine, Wakayama Medical University, Wakayama, Japan

[2] Department of Microbiology and Molecular Genetics, Mie University Graduate School of Medicine, Mie, Japan

Introduction

Influenza virus, rhinovirus, coronavirus, parainfluenza virus, respiratory syncytia virus, and adenovirus are major etiological agents of acute respiratory disease. Since many of these respiratory viruses co-circulate around the same time, often in winter, there is an increasing possibility that dual or multiple viruses coinfect a single host [1]. Indeed, incidents of coinfection with multiple viruses were detected using multi-target analysis such as multiplex PCR or next-generation sequencing [2–7]. Several studies indicate that coinfection is not associated with disease outcome [5, 8–10], while others indicate increase of disease severity [11–13]. Thus, pathological relevance of coinfection is unclear.

Since respiratory viruses target epithelial cells in respiratory tract, coinfected viruses propagate at almost same region where they share their replication sites. In this context, it seems that growth of one virus affects that of other viruses in any way. Although virus–virus interactions have been recognized in vivo level [14–16], little has been reported on in vitro interactions of coinfected viruses. It has been assumed that single viruses cause virus-mediated respiratory diseases. Biological analysis of viral pathogens in the laboratory is almost always conducted in the absence of other viruses. Therefore, in vitro interactions of multiple viruses, especially respiratory viruses, are an interesting subject to be solved.

Influenza A virus (IAV) and human parainfluenza virus type 2 (hPIV2) are common pathogens that cause community-acquired respiratory disease in the same epidemic season, usually in winter. Both of these negative-stranded RNA viruses utilize sialic acids on the cell surface as a receptor, allowing them to target same cells. However, their biological properties are quite different. The IAV genome

consists of eight segments that replicate in the nucleus. In contrast, hPIV2 has a non-segmented genome, and its replication is primarily in the cytoplasm. Both viruses carry a system to evade host antiviral responses. The non-structural (NS1) protein of IAV has been reported to limit interferon (IFN) production by blocking the retinoic acid-inducible gene I (RIG-I)/interferon-beta promoter stimulator 1 (IPS-1) signaling pathway [17]. Also it blocks the function of IFN-induced proteins, such as 2′–5′-oligoadenylate synthetase and the dsRNA-dependent serine/threonine protein kinase R [18–21]. The counterpart of hPIV2 is the V protein. The V protein inhibits IFN production by binding to RIG-I like receptors, the melanoma differentiation-associated gene 5 (MDA5) and laboratory of genetics and physiology 2 (LGP2) [22, 23]. The V protein also acts as an alternative substrate for inhibitor of kappa B kinase epsilon and TRAF family member-associated NF-kappa-B activator binding kinase 1 leading to inhibition of the interferon regulatory transcription factor (IRF) 3 activation [24]. The V protein also inhibits Toll-like receptor (TLR) 7- and TLR 9-dependent signaling by interaction with the IRF 7 and the tumor necrosis factor receptor-associated factor 6 (TRAF6) [25]. In addition, the V protein suppresses expression of the interferon inducible genes by degradation of the signal transducer and activator of transcription 2 (STAT2) protein [26–29].

To explore how coinfection of different viruses affects their biological properties, we infected Vero cells with IAV and hPIV2 simultaneously, and their growth kinetics was analyzed. We found that the growth of IAV was enhanced by coinfection with hPIV2, but not vice versa. Further experiments revealed that the enhanced growth of IAV was attributed to generation of syncytia of IAV-infected cells induced by hPIV2 coinfection. We also confirmed that IAV growth was slightly increased by hPIV2-induced cell fusion in cells from the respiratory epithelium. These results suggest that viral propagation by coinfection with different viruses can modify their pathological consequences.

Materials and methods

Cells and viruses

Africa green monkey kidney (Vero) cells were maintained in Eagle's minimal essential medium (MEM) containing 10 % fetal calf serum (FCS). Madin–Darby canine kidney (MDCK) cells were maintained in MEM containing 5 % newborn calf serum. Human alveolar epithelial (A459) cells and human bronchioalveolar carcinoma (H358) cells were maintained in Dulbecco's modified Eagle's medium containing 10 % FCS and RPMI 1640 medium containing 10 % FCS, respectively. All cells were maintained at 37 °C under 5 % CO_2. Influenza A virus (A/Puerto Rico/8/34, H1N1; referred to as IAV) was provided by Yoko Matsuzaki (Yamagata University) and was propagated in MDCK cells. Human parainfluenza virus type 2 (Toshiba strain; referred as to hPIV2) was propagated in Vero cells. The hPIV2-mutant virus H-83/186 was described previously [30]. All virus stocks were stored at −80 °C until use.

Antibodies

Anti-P/V protein (315-1), anti-HN protein (M1-1A, 42S1), and anti-F protein (144-1A) of human parainfluenza virus type 2 monoclonal antibodies (MAbs) were previously reported [31, 32]. Rabbit serum against influenza A virus (H1N1) was provided by Yoshihiro Kawaoka (Institute of Medical Sciences, University of Tokyo). Anti-Stat1 (N terminus) MAb and anti-Stat2 (c-20) rabbit polyclonal antibody were purchased from BD Biosciences and Santa Cruz Biotechnology, respectively.

Viral growth assay

Vero cells cultured in a 12-well plate were inoculated with IAV, hPIV2, or a mixture of IAV and hPIV2 at a multiplicity of infection (MOI) of 0.01. The infected cells were incubated in MEM containing 0.2 % bovine serum albumin (BSA) and 0.5 μg/ml TPCK-trypsin (Worthington Biochemical). The culture supernatants were harvested at 24, 48, and 72 h after infection. In a particular condition, which inhibited multiple rounds of IAV replication, the infected cells were incubated without TPCK-trypsin or with 5 mM ammonium chloride. In case of infection for A549 or H358 cells, IAV and hPIV2 were inoculated at an MOI of 1 and 0.05, respectively. Then the infected cells were incubated in TPCK-trypsin-free medium for 48 h.

Virus titration

The plaque assay was employed to quantitate IAV. Briefly, MDCK cells in a six-well pate were infected with viruses and cultured in MEM containing 0.3 % BSA, 0.5 μg/ml TPCK-trypsin, and 1 % agarose for 36–48 h until plaques were visible. For hPIV2, the 50 % tissue culture infectious dose ($TCID_{50}$) assay was employed using a 24-well plate. Briefly, Vero cell suspensions in wells of a plate were simultaneously mixed with tenfold serial dilutions of virus and then cultured in MEM with 10 % FCS for 4–5 days. Virus infection was confirmed by microscopic examination of cytopathic effect and $TCID_{50}$ was calculated using the Reed and Muench method [33].

Immunofluorescent staining assay (IFA)

The cultured cells were washed twice with phosphate-buffered saline (PBS) and fixed with 4 % paraformaldehyde in PBS for 15 min. The cells were then permeabilized with 0.2 % Triton X-100 in PBS for 15 min. The cells were incubated with a primary antibody and washed three times with 0.05 % Tween 20 in PBS (PBS-T). Next, the cells were incubated with secondary antibodies [Alexa Fluor 488 goat anti-mouse IgG (H + L) for mouse monoclonal antibody, or Alexa Fluor 594 goat anti-rabbit IgG (H + L) for rabbit anti-serum (Invitrogen)] and washed with three changes of PBS-T. Cell nuclei were counterstained with Hoechst 33342 (Invitrogen). Immunofluorescent stained cells were analyzed using a fluorescent microscope.

Western blot analysis

Sodium dodecyl sulfate–polyacrylamide gel electrophoresis (SDS-PAGE) and western blots were performed according to standard procedures. The cells were lysed in lysis buffer [50 mM Tris-HCl pH 8.0, 150 mM NaCl, 0.6 % octylphenoxypolyethoxyethanol (IGEPAL CA-630), 1 mM EDTA] and separated on a 7.5 or 10 % Tris–glycine gel, and then transferred to a nitrocellulose membrane. Blots were blocked with 5 % skim milk in PBS and incubated with a primary antibody and washed three times with PBS-T. Next, the blots were incubated with peroxidase-labeled horse anti-mouse IgG (H + L) or peroxidase-labeled goat anti-rabbit IgG (H + L) (Vector Laboratories) and washed with three changes of PBS-T. They were then visualized by using ImmunoCruz™ Western Blotting Luminol Reagent (Santa Cruz Biotechnology) according to the manufacturer's instructions. Images were captured with a cooled CCD camera.

Expression of viral proteins by plasmid transfection

For the transient expression of the hPIV2 HN, F, or HN and F proteins, Vero cells (1×10^5 cells in a 12-well plate) were transfected with the SRα expression plasmid [34] encoding the HN or the F glycoprotein [35, 36], or a mixture of both the plasmids by using FuGENE HD transfection reagent (Promega). The Vero cells constitutively expressing hPIV2 V protein (Vero-V) were established using the episomal Epstein–Barr virus-based expression system pEBS-V [27, 37]. The empty plasmid pEBS-PL [37] was used for the control cells (Vero-E). The transfected cells were cultured with hygromycin B (0.25 mg/ml) and hygromycin B-resistant cells were pooled. Three cell pools obtained by three independent transfections were subjected to experiments.

Results

Growth of IAV is enhanced by coinfection with hPIV2

To investigate how coinfection of IAV and hPIV2 affects growth of each virus, Vero cells were infected with a mixture of IAV and hPIV2 at an MOI of 0.01, and growth kinetics of the coinfected viruses was compared with that of singly infected viruses. These experiments require that IAV or hPIV2 can be selectively detected in a mixture of both viruses. IAV induced little cytopathic effect in Vero cells cultured in the presence of serum whose protease inhibitors suppressed multiple replication of IAV, whereas hPIV2 produced extensive CPE. hPIV2, in contrast, was

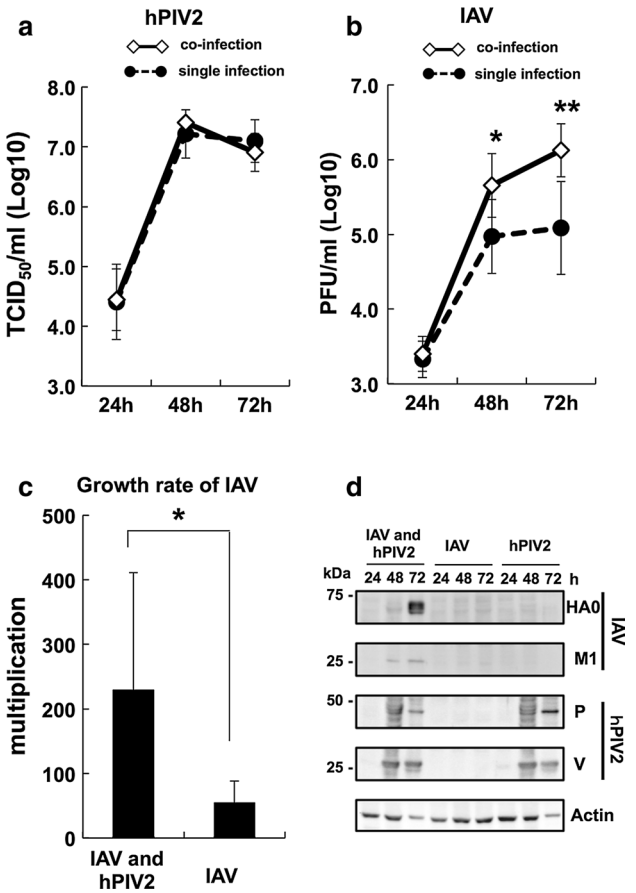

Fig. 1 Growth of IAV was enhanced by coinfection with hPIV2. **a** hPIV2 titers at each time points were measured by $TCID_{50}$ assay in Vero cells. *Open diamond* IAV and hPIV2 coinfection, *filled circle* hPIV2 single infection. **b** IAV titers at each time points were measured by plaque assay in MDCK cells, *Open diamond* IAV and hPIV2 coinfection, *filled circle* IAV single infection. **c** Growth rate of IAV was calculated by dividing the titer at 48 h by that at 24 h. **a**–**c** The data are shown as mean ± SD ($n = 7$). **, *$P < 0.05$ and $P < 0.01$, respectively, according to the Student's t test. **d** Production of viral polypeptides was analyzed by western blotting. The HA0 and M1 of IAV, and the V and P of hPIV2 were identified by their mobility

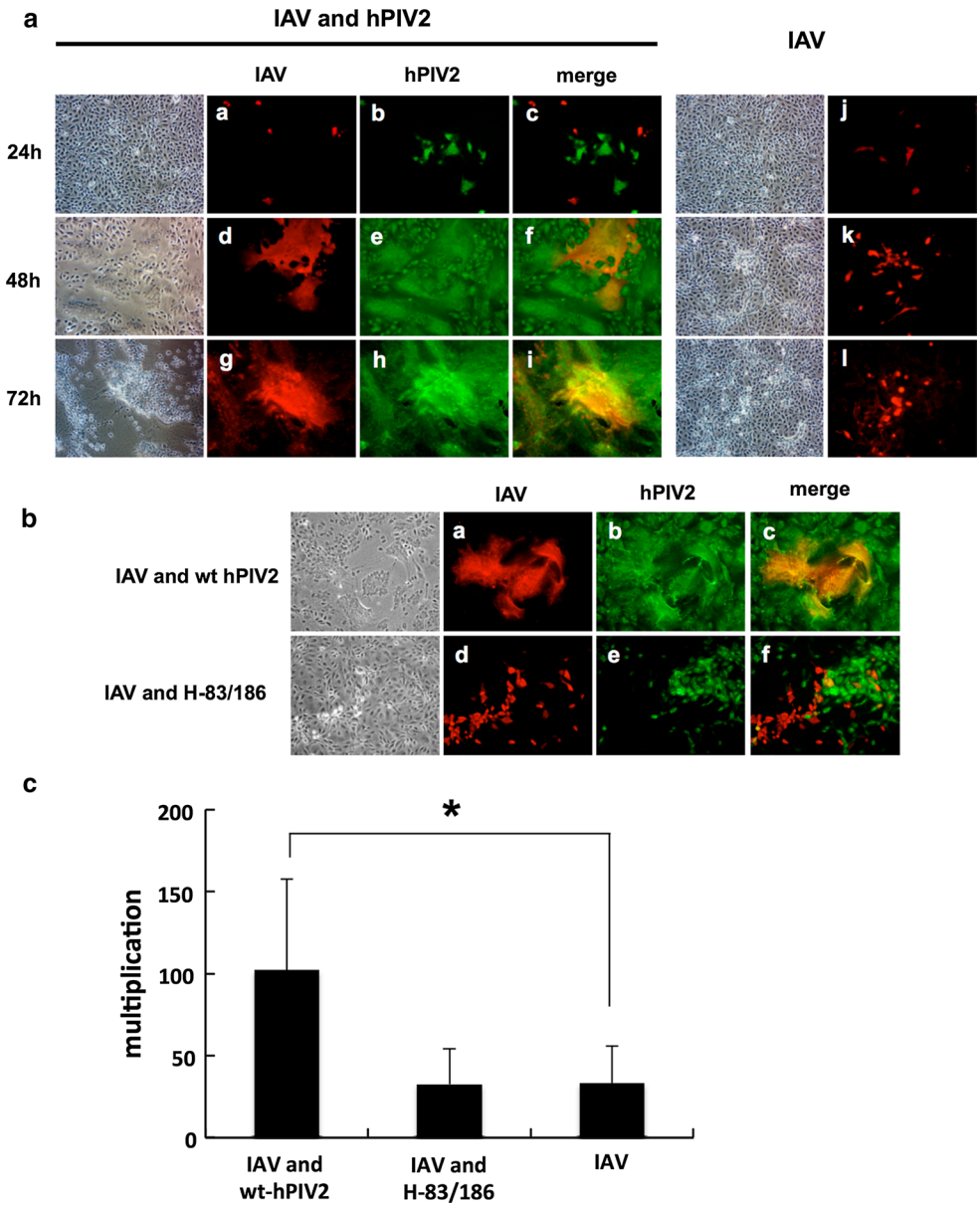

Fig. 2 IAV infection is expanded by cell fusion induced by hPIV2 infection. **a** IAV- and hPIV2-infected Vero cells were detected using a mixture of anti-IAV rabbit polyclonal antibody and anti-hPIV2 mouse MAbs. Alexa Fluor 594 goat anti-rabbit IgG (H + L) (*red*) and Alexa Fluor 488 goat anti-mouse IgG (H + L) (*green*) were used as secondary antibodies. **b** Vero cells coinfected with IAV and wt hPIV2 or IAV and H-83/186 hPIV2-mutant virus were detected at 48 h after infection in a manner similar to (**a**). **c** The growth rate of IAV from 24 to 48 h was calculated as described in Fig. 1. The data are shown as mean ± SD ($n = 6$). $^*P < 0.05$, according to the one-way ANOVA followed by the Dunnett's test

unable to produce plaques in MDCK cells under the same culture conditions as the conventional plaque assay for IAV (data not shown). Thus, we could employ the plaque and $TCID_{50}$ assays for quantitative determination of IAV and hPIV2, respectively.

Growth kinetics of hPIV2 during coinfection with IAV was identical to that of hPIV2 infection alone (Fig. 1a). On the other hand, IAV growth was enhanced by coinfection with hPIV2 at 48 and 72 h (Fig. 1b). Additionally, we calculated the growth rates of IAV from 24 to 48 h by dividing the virus titer at 48 h by that of 24 h and compared them between coinfection and single infection. This analysis revealed that IAV replication by coinfection with hPIV2 was significantly higher than that by single infection (Fig. 1c). The level of viral polypeptides in the infected cells correlated with growth kinetics of each virus (Fig. 1d). The P and V proteins of hPIV2 were equally synthesized regardless of whether Vero cells were singly infected or coinfected. In contrast, the HA0 and M1 proteins of IAV were detectable only in coinfected cells. In singly infected Vero cells, IAV replication was confirmed by IFA (Figs. 1b, 2a); nevertheless, the polypeptides of IAV were undetectable under the condition of western blotting we employed.

Cell fusion by hPIV2 supports efficient propagation of IAV

To explore why IAV growth was enhanced by coinfection with hPIV2, we observed virus spread in Vero cells by IFA using antibodies against each virus (Fig. 2a). At 24 h

after infection, the IAV- or hPIV2-infected cells were sporadically detected, and double-infected cells were rarely observed (Fig. 2a, panel c). At 48 h after infection, almost all cells were infected with hPIV2, and syncytia were extensively generated (Fig. 2a, panel e). It is noteworthy that widespread IAV antigens were detected in the syncytia at this time point (Fig. 2a, panel d), and the spreading pattern of IAV in coinfection was obviously distinguishable from that of single infection (Fig. 2a, panel k). Coinfection with hPIV2 induced the drastic expansion of the IAV infection, which correlated with increased growth rate of IAV by coinfection (Fig. 1c). At 72 h after infection, coinfection with hPIV2 expanded the area of IAV infection as cell fusion by hPIV2 infection proceeded (Fig. 2a, panel i).

Next, we used the hPIV2-mutant virus H-83/186 whose cell fusion activity was dramatically reduced due to two amino acid substitutions in the HN protein [30]. When Vero cells were coinfected with IAV and the H-83/186 hPIV2-mutant virus, we could hardly observe cell fusion at 48 h after infection, which contrasted markedly with extensive cell fusion induced by wild-type (wt) hPIV2 infection (Fig. 2b, panels b, e). The IAV-infected cells were found sporadically at 48 h after infection, which look like single IAV infection (Fig. 2a, panel k and b, panel d). The growth kinetics of H-83/186-mutant virus was almost identical with that of wt hPIV2 (data not shown). The growth rate of IAV in coinfection with wt hPIV2 from 24 to 48 h after infection resulted in about a threefold increase over that of a single IAV infection. In contrast, the growth rate of IAV was not increased by coinfection with the H-83/186-mutant virus and was identical with that of a single IAV infection (Fig. 2c). These results suggested that the enhanced propagation of IAV in hPIV2 coinfection was due to the generation of syncytia that incorporated IAV-infected cells.

Expression of the hPIV2 V protein does not participate in enhanced propagation of IAV

The V protein of hPIV2 plays a major role in counteracting cellular antiviral activity [22–29]. Since some of the targets of V protein are involved in an IFN-independent innate antiviral response [38–42], V may have some relevance to accelerated replication of IAV irrespective of inhibition of type I IFN expression. To test this possibility, we established Vero cells constitutively expressing the hPIV2 V protein (Vero-V) using the episomal Epstein–Barr virus-based expression system (Fig. 3a). Since pEBS-V was maintained in transfected cells as an episome, we eliminated untransfected cells using hygromycin B, and resistant cells were pooled as Vero-V cells. Vero-E control cells were generated by introduction of an empty plasmid. IFA of the Vero-V cells showed that, except for a small population, the majority of cells expressed the V protein, which localized

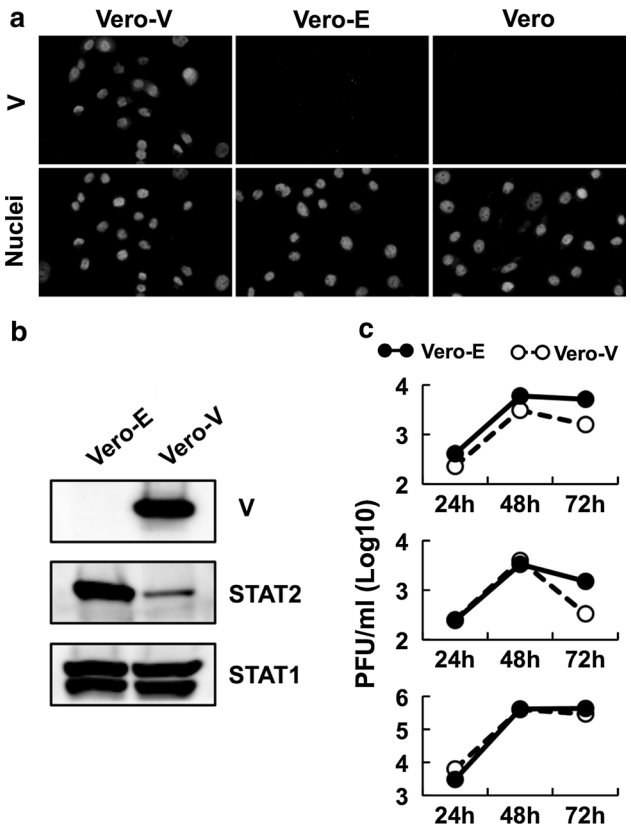

Fig. 3 V protein of hPIV2 has no influence on IAV growth. **a** V expression in the Vero-V cells was detected by IFA. Hoechst 33342 was used for a nuclear counterstain. **b** Expression level of the V, STAT1, and STAT2 were analyzed by western blotting. **c** The growth kinetics of IAV was studied in three Vero-V (*open circle*) or Vero-E (*filled circle*) cells which were established in independent transfections

predominantly in the nuclei as reported previously (Fig. 3a) [26, 43]. The functionality of expressed V protein was confirmed by STAT2 degradation in the Vero-V cells (Fig. 3b). The growth property of IAV was studied in three pools of Vero-V and Vero-E cells, which were established by independent transfections. V protein expression did not enhance the propagation of IAV in the three experiments (Fig. 3c), suggesting that V was not involved in the enhanced propagation of IAV during coinfection with hPIV2.

Cell fusion induced by the hPIV2 HN and F proteins is sufficient for enhanced propagation of IAV

To confirm that cell fusion by hPIV2 infection supported the enhanced propagation of IAV, we induced cell fusion by co-expression of the HN and F proteins of hPIV2. Vero cells were transfected with expression plasmids for the hPIV2 HN and F proteins and incubated for 10 h. The transfected cells were then infected with IAV at an MOI of 0.01, and the amount of IAV production was quantitated

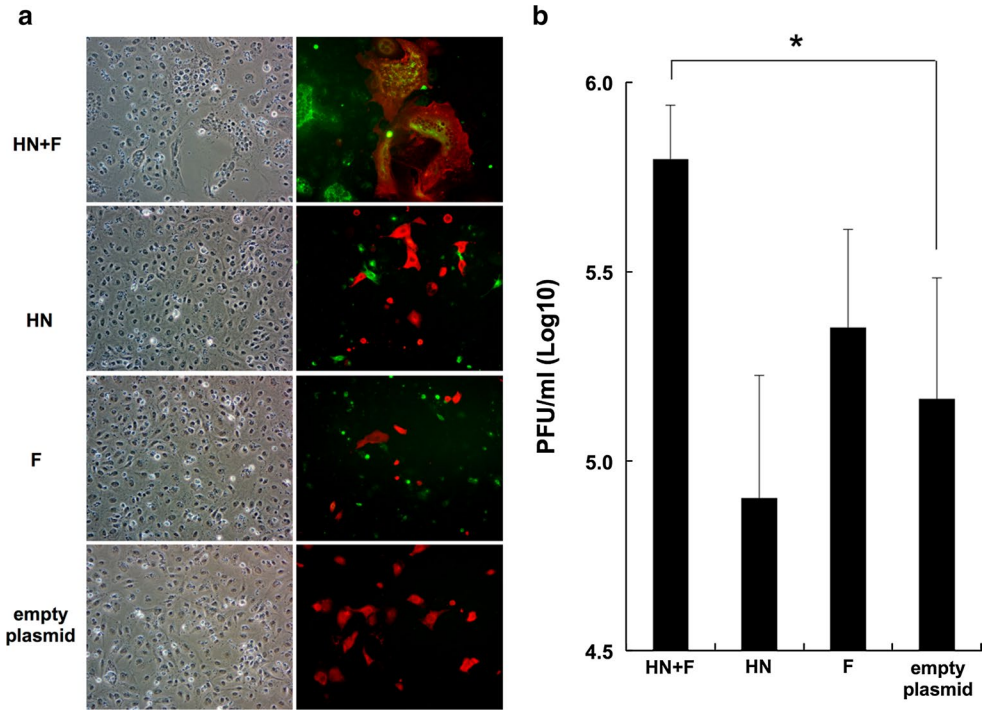

Fig. 4 Cell fusion is sufficient for enhanced growth of IAV. Vero cells were transfected with plasmids for expression of the hPIV2 HN and F proteins and then infected with IAV at an MOI of 0.01. **a** hPIV2 proteins expression (*green*) and IAV infection (*red*) were detected at 48 h after infection by IFA. **b** Virus titers at 48 h after infection were measured by plaque assay. The data are shown as mean ± SD ($n = 5$). *$P < 0.05$, according to the one-way ANOVA followed by the Dunnett's test

at 48 h after infection. Cell fusion was observed in Vero cells that co-expressed the HN and F proteins, but not in cells that expressed either the HN or F proteins by themselves, and IAV infection was detected in the syncytia (Fig. 4a). IAV propagated more efficiently in Vero cells that expressed the HN and F proteins than cells that expressed either the HN or F proteins (Fig. 4b). These results indicated that cell fusion of IAV-infected cells was the likely cause of the enhanced growth of IAV by coinfection with hPIV2.

Cell fusion induced by hPIV2 infection supports IAV production in cells originated from respiratory epithelium

Since the respiratory epithelium is primary target of IAV and hPIV2, human alveolar epithelium cell, A549, and human bronchioalveolar carcinoma cell, H358, were used for coinfection experiments. Cell fusion by hPIV2 infection at an MOI of 0.05 was observed in H358 cells but not in A549 cells (Fig. 5, panels d, k). The cell fusion activity of hPIV2 in H358 cells was apparently weak in comparison with that in Vero cells (Figs. 2a, panel e, 5, panel k). To maximize cell fusion effect in IAV production, we infected IAV at an MOI of 1 and incubated the infected cell without trypsin. Coinfection of hPIV2 decreased IAV production in A549 cells, but did not decrease in H358 cell (Table 1), indicating that coinfection with wt hPIV2 tended to support IAV production in H358 cells. To confirm the IAV productivity by hPIV2 coinfection was relevant to cell fusion, the reduced fusogenic-mutant virus, H-83/186, was used for coinfection with IAV as shown in Fig. 2b. Coinfection of the H-83/186 hPIV2 mutant had no effect on IAV production in H358 cells (Table 1, H358, H-83/186 hPIV2 mutant).

Coinfection with hPIV2 allows IAV to propagate in the conditions that inhibit multiple rounds of replication

Cell fusion enables IAV to spread to neighboring cells without infection by progeny viruses. Thus, the growth of IAV by coinfection with hPIV2 might be maintained under conditions that generally do not support IAV propagation. To test this hypothesis, we performed two experiments. First, Vero cells coinfected with IAV and hPIV2 were incubated in the absence of trypsin, which confers infectivity of progeny virus by cleavage of the influenza virus hemagglutinin (HA) [44, 45]. Second, ammonium chloride, which suppresses influenza virus entering the cytoplasm by inhibition of endosomal acidification [46–48], was added to culture medium at 3 h after infection. Neither treatment affected cell fusion and virus growth by hPIV2 infection (Fig. 6a, b). Under those conditions, the growth of IAV declined from 48–72 h in Vero cells infected with IAV alone, indicating that the treatments inhibited multiple rounds of IAV replication. Despite these same conditions, IAV continued to propagate when Vero cells were coinfected with hPIV2 (Fig. 6c).

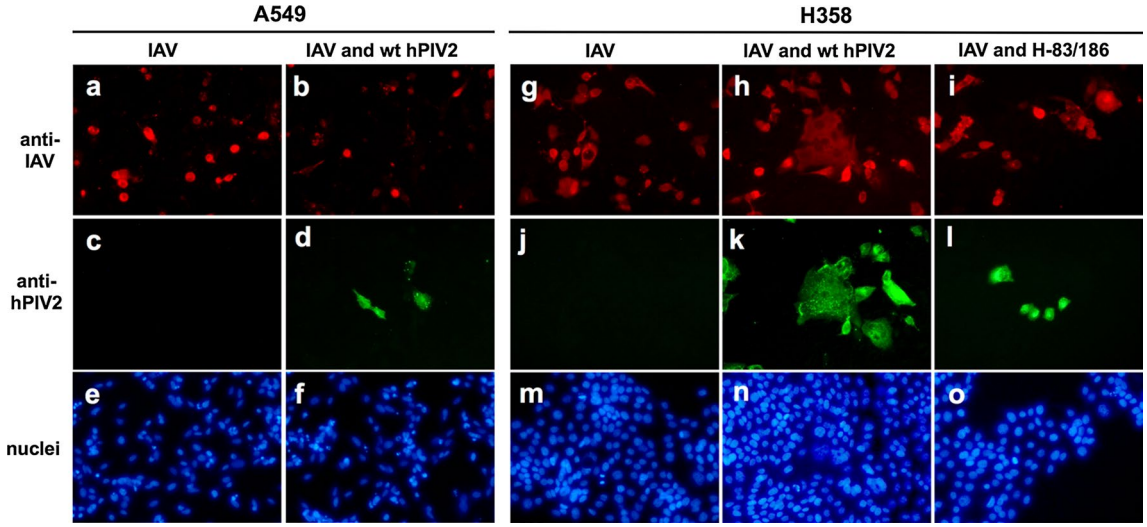

Fig. 5 Cell fusion is induced by hPIV2 infection in cells originated from the respiratory epithelium. A549 and H358 cells were infected with indicated viruses and incubated for 48 h. Culture supernatants were subjected to virus titration (Table 1). Virus infected cells were detected by IFA using the same method as in Fig. 2. Hoechst 33342 was used for a nuclear counterstain

Table 1 IAV production by hPIV2 coinfection

Cell	Type of hPIV2	Single infection	Coinfection	
		IAV[a]	IAV[a]	hPIV2[b]
A549	wt hPIV2	4.1×10^6	3.1×10^6	1.5×10^5
H358	wt hPIV2	6.6×10^6	7.1×10^6	1.3×10^5
	H-83/186 hPIV2 mutant	2.9×10^6	2.8×10^6	1.5×10^5

Culture supernatants were recovered at 48 h after infection to titrate IAV

All titers were average of three independent experiments

[a] IAV titers were determined by the plaque assay in MDCK cells and shown as PFU/ml

[b] hPIV2 titers were determined by the $TCID_{50}$ assay in Vero cells and shown as $TCID_{50}$/ml

Discussion

Given the recent reports of respiratory tract infection with multiple viruses, it is of interest to examine the biological properties of a virus during coinfection with other viruses in vitro. In this study, we examined the coinfection of IAV and hPIV2 in cultured cells and showed that growth of IAV was enhanced by coinfection with hPIV2.

Why did hPIV2 coinfection enhance the growth of IAV in Vero cells? IAV growth reached a plateau at 48 h after infection in Vero cells (Fig. 1b), as the number of infected cells increased very little from 48 to 72 h after infection even though uninfected cells still existed (Fig. 2a, panels k, l). The inefficient spread of IAV in Vero cells limits the growth of IAV. When IAV was coinfected with hPIV2, hPIV2 induced extensive syncytia which incorporated the IAV-infected cells (Fig. 2a). Our results indicate that IAV could expand the infection due to cell fusion independently of infection by progeny viruses. It seems that formation of the IAV-infected syncytia overcame inefficient spread of IAV in Vero cells. This conclusion is supported by the fact that coinfection with the limited fusogenic H-83/186 hPIV2-mutant virus did not enhance the IAV growth (Fig. 2b) and that induction of cell fusion by the HN and F expression increased IAV production (Fig. 4b).

Both IAV and hPIV2 target the respiratory epithelium. As A549 and H358 cells are carcinoma cell lines originated from human respiratory epithelium and frequently used as in vitro model of the respiratory infection for IAV, we used these cells for coinfection experiments. Coinfection of hPIV2 resulted in limited cell fusion in H358 cells and IAV production was increased slightly. IAV cannot undergo multiple rounds of infection in cells incubated without trypsin. The slight increase in IAV production is presumably due to cell fusion induced by hPIV2. Indeed, the propagation of IAV was not impacted in A549 cells coinfected with wt hPIV2 and H358 cells coinfected with H-83/136 hPIV2-mutant virus, both of which lacked cell fusion. Thus, these results also support a hypothesis that IAV production correlates with cell fusion induced by hPIV2. Although these results suggest that cell fusion by hPIV2 infection supports IAV growth in the respiratory epithelium, further studies, such as the use of human primary airway epithelial cells, are essential to detailed evaluation of its significance.

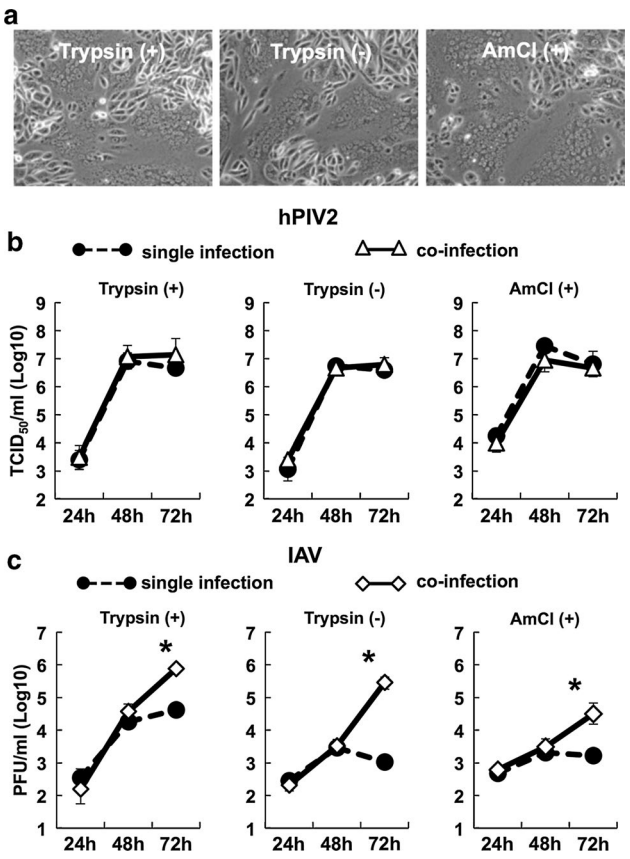

Fig. 6 Cell fusion enables IAV to grow in the condition that generally inhibits propagation of IAV. After virus adsorption, the cells were incubated either in the absence of trypsin or in the presence of ammonium chloride (AmCl). **a** The extent of cell fusion under those conditions was observed by microscopy. **b** hPIV2 titers at each time points were measured by $TCID_{50}$ assay in Vero cells. *Open triangle* IAV and hPIV2 coinfection, *filled circle* hPIV2 single infection. **c** IAV titers at each time points were measured by plaque assay in MDCK cells, *Open diamond* IAV and hPIV2 coinfection, *filled circle* IAV single infection. **b**, **c** The data are shown as mean ± SD ($n = 3$). $^*P < 0.01$, according to the Student's *t* test

The growth of hPIV2 was not affected by IAV coinfection in Vero cells (Fig. 1a). This contrasts with the results by Shinjoh et al. [49], who showed that IAV coinfection suppressed growth of respiratory syncytial virus (RSV) in MDCK cells. In MDCK cells, IAV highly efficiently replicates and induces severe cytopathic effect. Therefore, the cytopathogenicity of IAV is predicted as a major cause of growth suppression of RSV. In contrast, it seems that hPIV2 replication was not suppressed because IAV infection showed little cytopathic effect in Vero cells (Fig. 2a). This prediction is supported by our preliminary experiment, in which growth of hPIV2 with IAV coinfection was reduced to 1/10–1/30 of that of hPIV2 infection alone in MDCK cells (data not shown).

The paramyxovirus V protein is a multifunctional protein that counteracts the cellular antiviral system [22–29]. Although almost all the targets of the V protein are key molecules in type I IFN induction or IFN signaling, some of the targets are capable of inducing innate antiviral response independent of IFN [38–42]. These findings raise the possibility that the V protein counteracts the cellular antiviral system even in type I IFN gene-deficient Vero cells [50]. Thus, we examined whether the V protein of hPIV2 had an impact on intracellular replication of IAV in IAV and hPIV2-coinfected Vero cells. We established Vero cells constitutively expressing the hPIV2 V protein and showed that the localization of the V protein was predominantly intranuclear in Vero-V cells (Fig. 3a). Our results indicated that the expression of V protein alone did not enhance IAV growth, suggesting that the antiviral factors are unlikely to be involved in IAV replication. In addition, the intranuclear V protein conceivably has no effect on IAV genome replication. Although the functionality of the expressed V protein was confirmed by degradation of STAT2 protein, these results may be misleading. Our results agreed with the previous report indicating intranuclear localization of the V protein in the V protein-expressing cells [26, 43]. The V protein, however, exhibited not only intranuclear distribution but also distribution throughout the cytoplasm in hPIV2-infected cells [51]. Thus, the V protein in Vero-V cells may not be functionally equivalent to that in hPIV2-infected cells. Indeed, V protein expression in our cells does not complement impaired replication of a mutant hPIV2 due to amino acid substitutions in the V protein [52]. Accordingly, there is still a possibility that the V protein supports the enhanced IAV growth in coinfected cells.

The distinct growth properties of IAV during hPIV2 coinfection were clearly demonstrated by infections in the absence of trypsin or in the presence of ammonium chloride. To acquire infectivity of IAVs, the HA protein must be activated by trypsin cleavage at a specific site. Ammonium chloride inhibits acidification of endosomes where a low-pH-dependent conformational change in the HA protein triggers fusion of the virus envelope with the endosomal membrane [46]. Thus, in either condition multiple rounds of IAV replication are suppressed. We found that the titer of IAV decreased after 48 h after infection in the case of single infection (Fig. 5c). However, IAV continued to grow under these conditions when hPIV2 was coinfected. The distinct growth of IAV is presumed to be largely attributable to cell fusion induced by hPIV2. As discussed above IAV could expand the extent of infection by the cell fusion independently of infection by progeny viruses. Therefore, syncytium formation could confer expanded region of virus production to IAV regardless of culture condition. From this perspective, viruses with the ability to induce syncytium formation, such as RSV and mumps virus, may support IAV propagation as seen in this study.

Our results suggest that a virus can acquire additional properties when other viruses are present in the same tissue. Since multiple virus infections, especially in respiratory and intestinal tracts, are not uncommon, virus–virus interaction may well be an important determinant of pathological consequences. Therefore, in addition to conventional analyses that focus on a single virus infection, an analysis of coinfection by dual or multiple viruses should be conducted.

Acknowledgments We thank Yoko Matsuzaki for kindly providing us with influenza A virus A/Puerto Rico/8/24 and Yoshihiro Kawaoka for providing us with the rabbit antiserum against influenza A virus. This work was supported by JSPS KAKENHI Grant Number 15K08500.

References

1. Drews AL, Atmar RL, Glezen WP, Baxter BD, Piedra PA, Greenberg SB (1997) Dual respiratory virus infections. Clin Microbiol Infect 25:1421–1429. doi:10.1086/516137
2. Arden KE, McErlean P, Nissen MD, Sloots TP, Mackay IM (2006) Frequent detection of human rhinoviruses, paramyxoviruses, coronaviruses, and bocavirus during acute respiratory tract infections. J Med Virol 78:1232–1240. doi:10.1002/jmv.20689
3. Bonroy C, Vankeerberghen A, Boel A, De Beenhouwer H (2007) Use of a multiplex real-time PCR to study the incidence of human metapneumovirus and human respiratory syncytial virus infections during two winter seasons in a Belgian paediatric hospital. Clin Microbiol Infect 13:504–509. doi:10.1111/j.1469-0691.2007.01682.x
4. Huguenin A, Moutte L, Renois F, Leveque N, Talmud D, Abely M, Nguyen Y, Carrat F, Andreoletti L (2012) Broad respiratory virus detection in infants hospitalized for bronchiolitis by use of a multiplex RT-PCR DNA microarray system. J Med Virol 84:979–985. doi:10.1002/jmv.23272
5. Renois F, Talmud D, Huguenin A, Moutte L, Strady C, Cousson J, Lévêque N, Andréoletti L (2010) Rapid detection of respiratory tract viral infections and coinfections in patients with influenza-like illnesses by use of reverse transcription-PCR DNA microarray systems. J Clin Microbiol 48:3836–3842. doi:10.1128/JCM.00733-10
6. Templeton KE, Scheltinga SA, Beersma MFC, Kroes ACM, Claas ECJ (2004) Rapid and sensitive method using multiplex real-time PCR for diagnosis of infections by influenza A and influenza B viruses, respiratory syncytial virus, and parainfluenza viruses 1, 2, 3, and 4. J Clin Microbiol 42:1564–1569. doi:10.1128/JCM.42.4.1564-1569.2004
7. Wylie KM, Mihindukulasuriya KA, Sodergren E, Weinstock GM, Storch GA (2012) Sequence analysis of the human virome in febrile and afebrile children. PLoS ONE 7:e27735. doi:10.1371/journal.pone.0027735
8. De Paulis M, Gilio AE, Ferraro AA, Ferronato AE, do Sacramento PR, Botosso VF, Oliveira DB, Marinheiro JC, Hársi CM, Durigon EL, Vieira SE (2011) Severity of viral coinfection in hospitalized infants with respiratory syncytial virus infection. J Pediatr (Rio J) 87:307–313. doi:10.2223/JPED.2100
9. Goka E, Vallely P, Mutton K, Klapper P (2012) Influenza A viruses dual and multiple infections with other respiratory viruses and risk of hospitalisation and mortality. Influenza Other Respir Viruses 7:1079–1087. doi:10.1111/irv.12020
10. Subbarao EK, Griffis J, Waner JL (1989) Detection of multiple viral agents in nasopharyngeal specimens yielding respiratory syncytial virus (RSV). An assessment of diagnostic strategy and clinical significance. Diagn Microbiol Infect Dis 12:327–332. doi:10.1016/0732-8893(89)90098-9
11. Cilla G, Oñate E, Perez-Yarza EG, Montes M, Vicente D, Perez-Trallero E (2008) Viruses in community-acquired pneumonia in children aged less than 3 years old: high rate of viral coinfection. J Med Virol 80:1843–1849. doi:10.1002/jmv.21271
12. Richard N, Komurian-Pradel F, Javouhey E, Perret M, Rajoharison A, Bagnaud A, Billaud G, Vernet G, Lina B, Floret D, Paranhos-Baccalà G (2008) The impact of dual viral infection in infants admitted to a pediatric intensive care unit associated with severe bronchiolitis. Pediatr Infect Dis J 27:213–217. doi:10.1097/INF.0b013e31815b4935
13. Semple MG, Cowell A, Dove W, Greensill J, McNamara PS, Halfhide C, Shears P, Smyth RL, Hart CA (2005) Dual infection of infants by human metapneumovirus and human respiratory syncytial virus is strongly associated with severe bronchiolitis. J Infect Dis 191:382–386. doi:10.1086/426457
14. Debiaggi M, Canducci F, Ceresola ER, Clementi M (2012) The role of infections and coinfections with newly identified and emerging respiratory viruses in children. Virol J 9:247. doi:10.1186/1743-422X-9-247
15. Greer RM, McErlean P, Arden KE, Faux CE, Nitsche A, Lambert SB, Nissen MD, Sloots TP, Mackay IM (2009) Do rhinoviruses reduce the probability of viral co-detection during acute respiratory tract infections? J Clin Virol 45:10–15. doi:10.1016/j.jcv.2009.03.008
16. Martin ET, Kuypers J, Wald A, Englund JA (2011) Multiple versus single virus respiratory infections: viral load and clinical disease severity in hospitalized children. Influenza Other Respir Viruses 6:71–77. doi:10.1111/j.1750-2659.2011.00265.x
17. Pichlmair A, Schulz O, Tan CP, Näslund TI, Liljeström P, Weber F, Reis e Sousa C (2006) RIG-I-mediated antiviral responses to single-stranded RNA bearing 5′-phosphates. Science 314:997–1001. doi:10.1126/science.1132998
18. Melville MW, Hansen WJ, Freeman BC, Welch WJ, Katze MG (1997) The molecular chaperone hsp40 regulates the activity of P58IPK, the cellular inhibitor of PKR. Proc Natl Acad Sci USA 94:97–102
19. Min JY, Krug RM (2006) The primary function of RNA binding by the influenza A virus NS1 protein in infected cells: inhibiting the 2′–5′ oligo (A) synthetase/RNase L pathway. Proc Natl Acad Sci USA 103:7100–7105. doi:10.1073/pnas.0602184103
20. Lu Y, Wambach M, Katze MG, Krug RM (1995) Binding of the influenza virus NS1 protein to double-stranded RNA inhibits the activation of the protein kinase that phosphorylates the eIF-2 translation initiation factor. Virology 214:222–228. doi:10.1006/viro.1995.9937
21. Li S, Min JY, Krug RM, Sen GC (2006) Binding of the influenza A virus NS1 protein to PKR mediates the inhibition of its activation by either PACT or double-stranded RNA. Virology 349:13–21. doi:10.1016/j.virol.2006.01.005
22. Andrejeva J, Childs KS, Young DF, Carlos TS, Stock N, Goodbourn S, Randall RE (2004) The V proteins of paramyxoviruses bind the IFN-inducible RNA helicase, mda-5, and inhibit its activation of the IFN-beta promoter. Proc Natl Acad Sci USA 101:17264–17269. doi:10.1073/pnas.0407639101
23. Childs K, Randall R, Goodbourn S (2012) Paramyxovirus V proteins interact with the RNA helicase LGP2 to inhibit RIG-I-dependent interferon induction. J Virol 86:3411–3421. doi:10.1128/JVI.06405-11
24. Lu LL, Puri M, Horvath CM, Sen GC (2008) Select paramyxoviral V proteins inhibit IRF3 activation by acting as alternative

substrates for inhibitor of kappaB kinase epsilon (IKKe)/TBK1. J Biol Chem 283:14269–14276. doi:10.1074/jbc.M710089200
25. Kitagawa Y, Yamaguchi M, Zhou M, Nishio M, Itoh M, Gotoh B (2013) Human parainfluenza virus type 2 V protein inhibits TRAF6-mediated ubiquitination of IRF7 to prevent TLR7- and TLR9-dependent interferon induction. J Virol 87:7966–7976. doi:10.1128/JVI.03525-12
26. Nishio M, Tsurudome M, Ito M, Kawano M, Komada H, Ito Y (2001) High resistance of human parainfluenza type 2 virus protein-expressing cells to the antiviral and anti-cell proliferative activities of alpha/beta interferons: cysteine-rich V-specific domain is required for high resistance to the interferons. J Virol 75:9165–9176. doi:10.1128/JVI.75.19.9165-9176.2001
27. Nishio M, Tsurudome M, Ito M, Garcin D, Kolakofsky D, Ito Y (2005) Identification of paramyxovirus V protein residues essential for STAT protein degradation and promotion of virus replication. J Virol 79:8591–8601. doi:10.1128/JVI.79.13.8591-8601.2005
28. Parisien JP, Lau JF, Rodriguez JJ, Sullivan BM, Moscona A, Parks GD, Lamb RA, Horvath CM (2001) The V protein of human parainfluenza virus 2 antagonizes type I interferon responses by destabilizing signal transducer and activator of transcription 2. Virology 283:230–239. doi:10.1006/viro.2001.0856
29. Ulane CM, Horvath CM (2002) Paramyxoviruses SV5 and HPIV2 assemble STAT protein ubiquitin ligase complexes from cellular components. Virology 304:160–166. doi:10.1006/viro.2002.1773
30. Tsurudome M, Nishio M, Ito S, Tanahashi S, Kawano M, Komada H, Ito Y (2008) Effects of hemagglutinin-neuraminidase protein mutations on cell–cell fusion mediated by human parainfluenza type 2 virus. J Virol 82:8283–8295. doi:10.1128/JVI.00460-08
31. Nishio M, Tsurudome M, Ito M, Watanabe N, Kawano M, Komada H, Ito Y (1997) Human parainfluenza virus type 2 phosphoprotein: mapping of monoclonal antibody epitopes and location of the multimerization domain. J Gen Virol 78:1303–1308. doi:10.1099/0022-1317-78-6-1303
32. Tsurudome M, Nishio M, Komada H, Bando H, Ito Y (1989) Extensive antigenic diversity among human parainfluenza type 2 virus isolates and immunological relationships among paramyxoviruses revealed by monoclonal antibodies. Virology 171:38–48. doi:10.1016/0042-6822(89)90508-4
33. Reed LJ, Muench H (1938) A simple method of estimating fifty per cent endopoints. Am J Epidemiol 27:493–497
34. Takebe Y, Seiki M, Fujisawa J, Hoy P, Yokota K, Arai K, Yoshida M, Arai N (1988) SR alpha promoter: an efficient and versatile mammalian cDNA expression system composed of the simian virus 40 early promoter and the R-U5 segment of human T-cell leukemia virus type 1 long terminal repeat. Mol Cell Biol 8:466–472. doi:10.1128/MCB.8.1.466
35. Tsurudome M, Kawano M, Yuasa T, Tabata N, Nishio M, Komada H, Ito Y (1995) Identification of regions on the hemagglutinin-neuraminidase protein of human parainfluenza virus type 2 important for promoting cell fusion. Virology 213:190–203. doi:10.1006/viro.1995.1559
36. Tsurudome M, Ito M, Nishio M, Kawano M, Okamoto K, Kusagawa S, Komada H, Ito Y (1998) Identification of regions on the fusion protein of human parainfluenza virus type 2 which are required for haemagglutinin-neuraminidase proteins to promote cell fusion. J Gen Virol 79:279–289. doi:10.1099/0022-1317-79-2-279
37. Bontron S, Ucla C, Mach B, Steimle V (1997) Efficient repression of endogenous major histocompatibility complex class II expression through dominant negative CIITA mutants isolated by a functional selection strategy. Mol Cell Biol 17:4249–4258
38. Nakaya T, Sato M, Hata N, Asagiri M, Suemori H, Noguchi S, Tanaka N, Taniguchi T (2001) Gene induction pathways mediated by distinct IRFs during viral infection. Biochem Biophys Res Commun 283:1150–1156. doi:10.1006/bbrc.2001.4913
39. Grandvaux N, Servant MJ, tenOever B, Sen GC, Balachandran S, Barber GN, Lin R, Hiscotto J (2002) Transcriptional profiling of interferon regulatory factor 3 target genes: direct involvement in the regulation of interferon-stimulated genes. J Virol 76:5532–5539. doi:10.1128/jvi.76.11.5532-5539.2002
40. Alazawi W, Heath H, Waters JA, Woodfin A, O'Brien AJ, Scarzello AJ, Ma B, Lopez-Otalora Y, Jacobs M, Petts G, Goldin RD, Nourshargh S, Gamero AM, Foster GR (2013) Stat2 loss leads to cytokine-independent, cell-mediated lethality in LPS-induced sepsis. Proc Natl Acad Sci USA 110:8656–8661. doi:10.1073/pnas.1221652110
41. Bose S, Kar N, Maitra R, DiDonato JA, Banerjee AK (2003) Temporal activation of NF-kappaB regulates an interferon-independent innate antiviral response against cytoplasmic RNA viruses. Proc Natl Acad Sci USA 100:10890–10895
42. Chew T, Noyce R, Collins SE, Hancock MH, Mossman KL (2009) Characterization of the interferon regulatory factor 3-mediated antiviral response in a cell line deficient for IFN production. Mol Immunol 46:393–399. doi:10.1016/j.molimm.2008.10.010
43. Watanabe N, Kawano M, Tsurudome M, Nishio M, Ito M, Ohgimoto S, Suga S, Komada H, Ito Y (1996) Binding of the V proteins to the nucleocapsid proteins of human parainfluenza type 2 virus. Med Microbiol Immunol 185:89–94. doi:10.1007/s004300050019
44. Klenk HD, Rott R, Orlich M, Blödorn J (1975) Activation of influenza A viruses by trypsin treatment. Virology 68:426–439. doi:10.1016/0042-6822(75)90284-6
45. Garten W, Bosch FX, Linder D, Rott R, Klenk HD (1981) Proteolytic activation of the influenza virus hemagglutinin: the structure of the cleavage site and the enzymes involved in cleavage. Virology 115:361–374. doi:10.1016/0042-6822(81)90117-3
46. Skehel JJ, Bayley PM, Brown EB, Martin SR, Waterfield MD, White JM, Wilson IA, Wiley DC (1982) Changes in the conformation of influenza virus hemagglutinin at the pH optimum of virus-mediated membrane fusion. Proc Natl Acad Sci USA 79:968–972
47. Sato SB, Kawasaki K, Ohnishi S (1983) Hemolytic activity of influenza virus hemagglutinin glycoproteins activated in mildly acidic environments. Proc Natl Acad Sci USA 80:3153–3157
48. Yoshimura A, Ohnishi S (1984) Uncoating of influenza virus in endosomes. J Virol 51:497–504
49. Shinjoh M, Omoe K, Saito N, Matsuo N, Nerome K (2000) In vitro growth profiles of respiratory syncytial virus in the presence of influenza virus. Acta Virol 44:91–97
50. Osada N, Kohara A, Yamaji T, Hirayama N, Kasai F, Sekizuka T, Kuroda M, Hanada K (2014) The genome landscape of the african green monkey kidney-derived vero cell line. DNA Res 21:673–683. doi:10.1093/dnares/dsu029
51. Nishio M, Tsurudome M, Ito M, Kawano M, Kusagawa S, Komada H, Ito Y (1999) Isolation of monoclonal antibodies directed against the V protein of human parainfluenza virus type 2 and localization of the V protein in virus-infected cells. Med Microbiol Immunol 188:79–82. doi:10.1007/s004300050108
52. Nishio M, Tsurudome M, Ishihara H, Ito M, Ito Y (2007) The conserved carboxyl terminus of human parainfluenza virus type 2 V protein plays an important role in virus growth. Virology 362:85–98. doi:10.1016/j.virol.2006.12.017